Structural Engineering and Mechanics, Vol. 5, No. 1 (1997) 69-83
DOI: http://dx.doi.org/10.12989/sem.1997.5.1.069

An efficient six-node plate bending hybrid/mixed element based on mindlin/reissner plate theory

Duan Mei†, Yutaka Miyamoto‡, Shoji Iwasaki‡† and Hideaki Deto‡†

Faculty of Civil Engineering, Iwate University, Ueda, 020 Morioka, Japan

Benkuan Zhou‡‡

Institute of Computational Engineering Science, Southwest Jiaotong University, Chengdu, China

Abstract. A new efficient hybrid/mixed thin~moderately thick plate bending element with 6-node (HM6-14) is formulated based on the Reissner-Mindlin plate bending theory. The convergence of this element is proved by error estimate theories and verified by patch test respectively. Numerical studies on such an element as HM6-14 demonstrate that it has remarkable convergence, invariability to geometric distorted mesh situations, to axial rotations, and to node positions, and no "locking" phenomenon in thin plate limit. The present element is suitable to many kinds of shape and thin~moderately thick plate bending problems. Further, in comparison with original hybrid/mixed plate bending element HP4, the present element yields an improvement of solutions. Therefore, it is an efficient element and suitable for the development of adaptive multi-field finite element method (FEM).

Key words: hybrid/mixed FEM; Mindlin/Reissner plate theory.

1. Introduction

It is known that the application of plates is widespread in practical engineering, so it is very important to find an efficient method which will overcome difficulties encountered in plate bending problems. The idea of plate bending for FEM was applied in the early sixties. At that time, the various difficulties that were encountered were not fully appreciated. For these reasons. the topic remains one in which research is active to the present day. To overcome shortcomings of displacement FEM, as the constraint condition a major problem for which a solution must still be found is approached for nearly incompressible materials and plate elements allowing for independent transverse displacement and cross-section rotations, hybrid stress FEM was initiated by professor Pian in 1964. In 1982 a new and more general method for formulating the assumed stress hybrid element was suggested by Pian and Chen, and hence, in principle, one could improve the properties of an element and enhance the solution accuracy. Based on this, they put forward a new formulation-Hybrid/Mixed finite element-in 1983. The birth and develop-

† Postgraduate Student
‡ Professor
‡† Assistant Professor
‡‡ Professor of Computational Mechanics

ment of hybrid/mixed FEM have a great deal of importance for the study of plate, shell and other problems. However, 6-node hybrid/mixed plate elements so far have not, to the authors' knowledge, been reported. A recent paper (Masa Hayashi, *et al.* 1993) about 6-node and 10-node element concerns, as a matter of fact, the series expansion method and not FEM. Analysis results were only similar to those of 8-node Serendipity displacement finite element which did not possess many of the qualities of the hybrid/mixed plate element. A study of 6-node hybrid/mixed plate element is necessary to develop adaptive multi-field FEM in which variable node elements are often used. The present study was undertaken with this background in mind.

The authors present a new hybrid/mixed element (HM6-14) based on the Reissner-Mindlin plate theory and the principle suggested by Pian, T.H.H. and Chen, D.P. in 1983, and prove its convergence according to error estimate theory and verify it based on the patch test. The calculated results show that HM6-14 has better convergence than 4-node hybrid/mixed element HP4, is free from "locking" effect in thin plate limit, insensitive to geomtric distortion and nearly invariable to axial rotations and node positions.

2. Variational formulation of hybrid/mixed FEM based on the Reissner/Mindlin theory

In this paper, 6-node quadrilateral element is deduced by the Reissner-Mindlin theory and the hyrid/mixed FEM.

2.1. Basic definitions

Firstly, basic definitions about displacement, stress and strain distributions are given as follows.

2.1.1. Displacement

$$u=\begin{Bmatrix} W \\ \theta_x \\ \theta_y \end{Bmatrix}=\begin{Bmatrix} W \\ \dfrac{\partial W}{\partial y}-Y_{yz} \\ -\dfrac{\partial W}{\partial x}+Y_{xz} \end{Bmatrix}=u_q+u_\lambda \tag{1}$$

Where W is transverse displacement in z direction, θ_x and θ_y represent the normal rotations about x and y directions, respectively, γ_{yz}, γ_{xz} are shearing strain components in rectangular coordinates, u_q, u_λ are compatible displacements in terms of nodal displacement q and incompatible displacement in terms of additional internal displacement parameters λ, respectively.

2.1.2. Strain

$$\varepsilon=\begin{Bmatrix} \varepsilon_f \\ \varepsilon_s \end{Bmatrix}=\begin{Bmatrix} D_f \\ D_s \end{Bmatrix}u \quad \text{where} \quad D_f=\begin{bmatrix} 0 & 0 & \dfrac{\partial}{\partial x} \\ 0 & -\dfrac{\partial}{\partial y} & 0 \\ 0 & -\dfrac{\partial}{\partial x} & \dfrac{\partial}{\partial y} \end{bmatrix} \quad D_s=\begin{bmatrix} \dfrac{\partial}{\partial x} & 0 & 1 \\ \dfrac{\partial}{\partial y} & -1 & 0 \end{bmatrix} \tag{2}$$

2.1.3. Stress

$$\sigma=\begin{Bmatrix} M \\ Q \end{Bmatrix}=\begin{Bmatrix} M_x \\ M_y \\ M_{xy} \\ Q_x \\ Q_y \end{Bmatrix} \tag{3}$$

Where M_x, M_y are bending moments in x and y directions respectively and M_{xy} is twisting moment with respect to the x axis.

2.2. Variational functional and finite element formulation

According to Pian, T.H.H. and Chen, D.P. (1983), the hybrid/mixed functional for an element may be written as:

$$\pi_R=\int_V\left[-\frac{1}{2}\sigma^T S\sigma+M^T(Du_q)-(D^T\sigma)^T u_\lambda\right]dV \tag{4}$$

where S is elastic compliance matrix. Substituting Eqs. (1), (2) and (3) into Eq. (4), we obtain the following equation.

$$\pi_R=\int_V\left[-\frac{1}{2}M^T S_f M-\frac{1}{2}Q^T S_s Q+M^T(Du_q)+Q^T(Du_q)-(D_f^T M)^T u_\lambda-(D_S{}^T Q)^T u_\lambda\right]dV \tag{5}$$

where

Assume $$S_f+S_s=S$$

$$M=P_f(x)\beta,\ Q=P_s(x)\beta,\ u_q=N(x)q,\ u_\lambda=Z(x)\lambda \tag{6}$$

When Eq. (6) is substituted into Eq. (5), function π_R can be written simply as

$$\pi_R=-\frac{1}{2}\beta^T(H_f+H_s)\beta+\beta^T(G_f+G_s)q-\beta^T(R_f+R_s)\lambda \tag{7}$$

in which

$$H_f=\int_V P_f^T S_f P_f dV\quad H_s=\int_V P_s^T S_s P_s dV\quad G_f=\int_V P_f^T(DN)dV\quad G_s=\int_V P_s^T(DN)dV$$

$$R_f=\int_V (D^T P_f)^T Z dV\quad R_s=\int_V (D^T P_s)^T Z dV$$

The stationary condition of π_R then yields that

$$K^{(e)}q=Q^{(e)},\quad \beta=H^{-1}Gq,\quad \sigma=PH^{-1}Gq$$

where

$$K^{(e)}=[\widetilde{G}_f+\widetilde{G}_s]^T[\widetilde{H}_f+\widetilde{H}_s]^{-1}[\widetilde{G}_f+\widetilde{G}_s]=\widetilde{G}^T\widetilde{H}^{-1}\widetilde{G},\ \widetilde{G}=G-R(R^TH^{-1}R)^{-1}R^TH^{-1}G,\ R=R_f+R_s$$

Table 1 Shape functions for the cases of Fig. 16 (II-VI).

	II	II, V, VI	IV
N_5	$0.5\times(1-\eta^2)(1+\xi)$	$0.5\times(1-\xi^2)$	$0.5\times(1-\eta^2)$
N_6	$0.5\times(1-\eta^2)(1-\xi)$	$0.5\times(1-\eta^2)$	$0.5\times(1-\xi^2)$

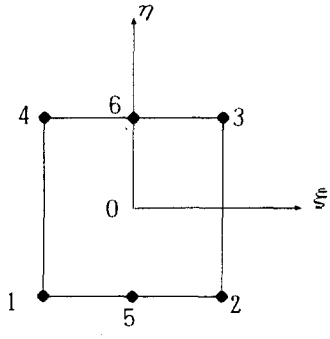

Fig. 1 A 6-node element under natural coordinate system (ξ, η).

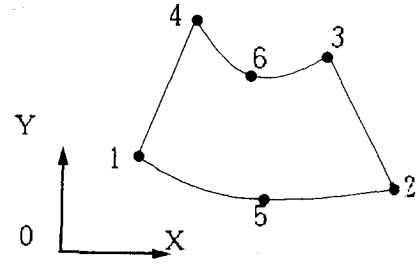

Fig. 2 A 6-node element under global coordinate system (x, y).

3. A 6-node quadrilateral hybrid/mixed plate bending element

Assume,

$$P_f(x)=\begin{bmatrix} 1 & x & y & 0 & 0 & 0 & 0 & 0 & 0 & xy & 0 & 0 & y^2 & x^2 \\ 0 & 0 & 0 & 0 & 1 & x & y & 0 & 0 & 0 & xy & 0 & x^2 & y^2 \\ 0 & 0 & 0 & 0 & 0 & 0 & 1 & x & y & 0 & 0 & xy & 0 & 0 \end{bmatrix}_{3\times 14}$$

$$P_s(x)=\begin{bmatrix} 0 & 1 & 0 & 0 & 0 & 0 & 0 & 0 & 1 & y & 0 & x & 0 & 2x \\ 0 & 0 & 0 & 0 & 0 & 1 & 0 & 1 & 0 & 0 & x & y & 0 & 2y \end{bmatrix}_{2\times 14} \tag{8}$$

$$N=[A_1, A_2, \cdots, A_6] \qquad A_i=\begin{bmatrix} N_i & 0 & 0 \\ 0 & N_i & 0 \\ 0 & 0 & N_i \end{bmatrix} (i=1, 2, \cdots, 6) \qquad \boldsymbol{q}=\{q_1, q_2, \cdots, q_{18}\}$$

$$\begin{aligned} N_i&=0.25\times(1+\xi_i\xi)(1+\eta_i\eta)-0.5\times(1-\xi^2)(1-\eta) \quad i=1, 2 \\ N_i&=0.25\times(1+\xi_i\xi)(1+\eta_i\eta)-0.5\times(1-\xi^2)(1+\eta) \quad i=3, 4 \end{aligned} \tag{9}$$

As shown in Fig. 1, we have

$$N_5=0.5\times(1-\xi^2)(1-\eta),\ N_6=0.5\times(1-\xi^2)(1+\eta)$$

but the shape functions are written as above Table 1 for the cases of Fig. 16 (II-VI).
where (ξ, η) is the natural coordinate.

$$Z(x)=0$$

Fig. 1 shows only a six-node element model. In fact this new element model contains certain

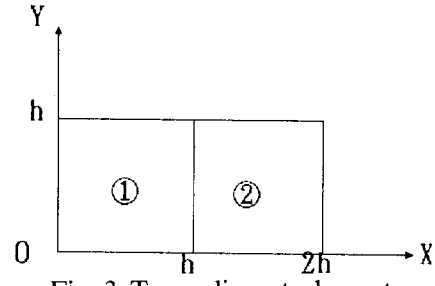

Fig. 3 Two adjacent elements.

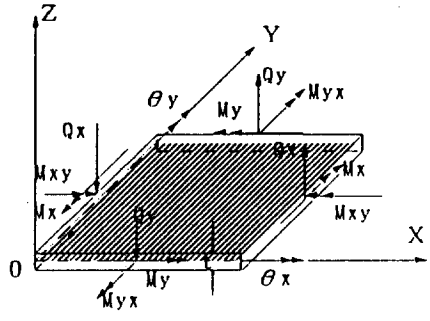

Fig. 4 Square plate and positive directions of bending moments and shearing forces.

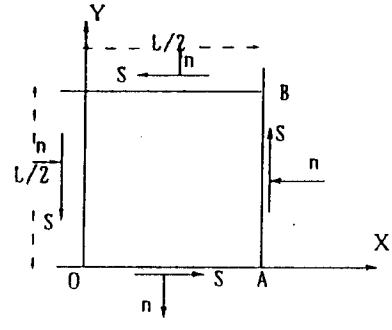

Fig. 5 The symmetric quadrant of the square plate.

generalizations which are explained in the following sections. The convergence is very important for a new element model, therefore, particular attention is given to this problem in the following section.

4. The verification and the proof of solution convergence

4.1. The patch test

The patch test has often been used in finite element formulation in order to verify the convergence quality of element. The ability of the element to maintain constant states of strain is an

essential requirement for achieving convergence to the exact solutions the finite element mesh is refined. As Fig. 6~Fig. 13 in the following section show, displacements and moments approach the exact solution as meshes are refined, confirming that the element passes the test. The patch test seems to be an efficient method which verifies the convergence of solution in engineering, but in the strict sense, it is neither a sufficient nor necessary condition for the convergence of solution (Stummel 1980, Zhong 1984). Therefore, the convergence of solutions for element HM6-14 will be proved by error estimate theories in the following section.

4.2. Proof of solution convergence based on error estimate theories

As can be easily seen, the matching of Eq. (8) and (9) leads to matrix G nonsigular, so the solution of hybrid/mixed finite element exists (Zhou and Duan 1993). For hybrid/mixed FEM, compatible displacement solution is continuous between elements; the continuity of stress solution is only in elements but not between elements. Therefore, it is necessary to consider stress error estimates on the boundary of adjacent elements whether or not they tend to zero as the size of meshes are within the limits. These are sufficient and necessary conditions for the convergence solution.

Def. 1 Reflection A_k is called k-linear if A_k: $X^k \rightarrow Y$ is linear for every variable $x_i (i=1, \cdots, k)$.

Def. 2 The norm of k-linear form $D^k \boldsymbol{u}(\boldsymbol{x})$ is defined as

$$\|D^K u(x)\| = \sup_{\substack{\|\xi_i\| \leq 1 \\ 1 \leq i \leq k}} \{|D^k u(\xi_1, \xi_2, \cdots, \xi_k)|$$

Let us consider adjacent elements, as shown in Fig. 3, without any loss of generality, where $*^{(1)}$, $*^{(2)}$ denote variations corresponding to element (1) and element (2) respectively.

$$\begin{aligned}
\sigma^{(1)} - \sigma^{(2)} &= P[H^{(1)-1} G^{(1)} - H^{(2)-1} G^{(2)}] q - P[H^{(1)-1} R^{(1)} - H^{(2)-1} R^{(2)}] \lambda \\
&= P[H^{(1)-1} (G^{(1)} - G^{(2)}) + (H^{(1)-1} - H^{(2)-1}) G^{(2)}] q \\
&\quad - P[H^{(1)-1} (R^{(1)} - R^{(2)}) + (H^{(1)-1} - H^{(2)-1}) R^{(2)}] \lambda \\
&= P[H^{(1)-1} (G^{(1)} - G^{(2)}) + H^{(1)-1} (H^{(2)} - H^{(1)}) H^{(2)-1} G^{(2)}] q \\
&\quad - P[H^{(1)-1} (R^{(1)} - R^{(2)}) + H^{(1)-1} (H^{(2)} - H^{(1)}) H^{(2)-1} R^{(2)}] \lambda
\end{aligned} \tag{10}$$

Since the matrixes which are given in this paper are composed of continuous functions, q exists, and H, G, R are bounded; therefore, there exists a generalized constant $C>0$ such that

$$\|\sigma^{(1)} - \sigma^{(2)}\| \leqq C (\|G^{(1)} - G^{(2)}\| + \|H^{(1)} - H^{(2)}\| + \|R^{(1)} - R^{(2)}\|)$$

Moreover

$$\begin{aligned}
G^{(1)} - G^{(2)} &= \int_{\Omega 1} P^T(x, y) DN(x, y) dA - \int_{\Omega 2} P^T(x, y) DN(x, y) dA \\
&= \int_0^h dy \int_0^h P^T(x, y) DN(x, y) dx - \int_0^h dy \int_h^{2h} P^T(x, y) DN(x, y) dx \\
&= \int_0^h dy \int_0^h P^T(x, y) DN(x, y) dx - \int_0^h dy \int_0^h P^T(x+h) DN(x+h, y) dx
\end{aligned}$$

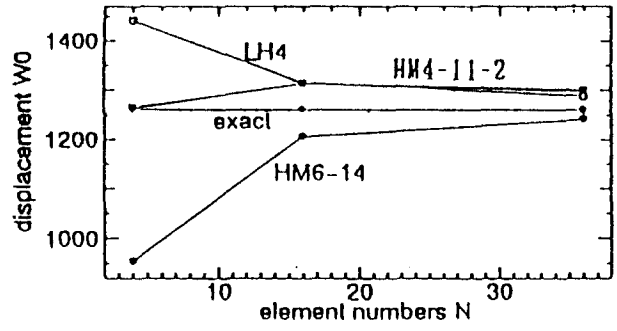

Fig. 6 Convergence of central displacement W_0 in the clamped plate under uniform loading (t=0.01).

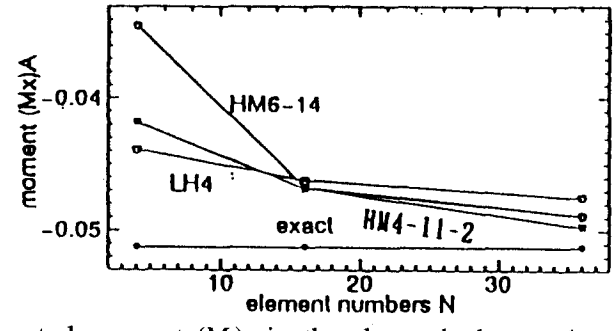

Fig. 7 Convergence of central moment $(M_x)_A$ in the clamped plate under uniform loading (t=0.01).

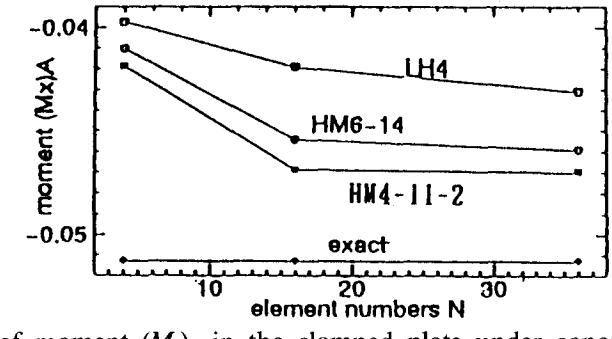

Fig. 8 Convergence of moment $(M_x)_A$ in the clamped plate under concentrated loading (t=0.2).

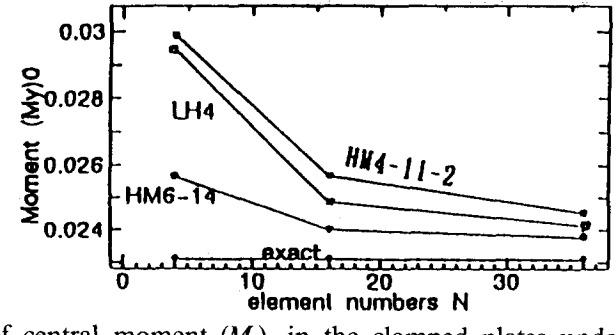

Fig. 9 Convergence of central moment $(M_y)_0$ in the clamped plates under uniform loading (t=0.2).

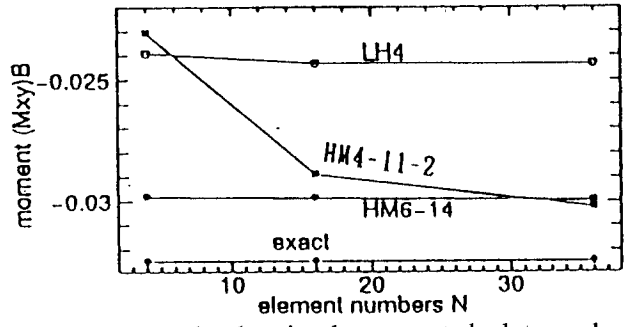

Fig. 10 Convergence of moment $(M_{xy})_B$ in the simply supported plate under uniform loading (t=0.01).

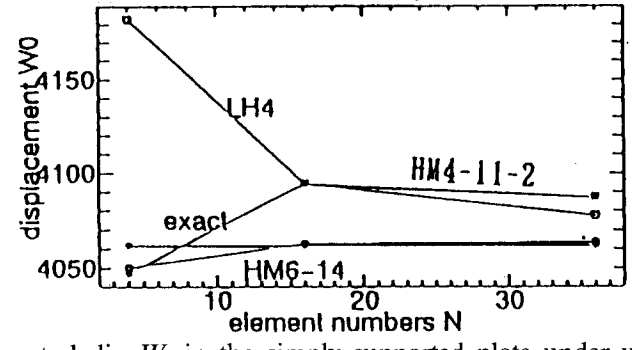

Fig. 11 Convergence of central dis. W_0 in the simply supported plate under uniform loading (t=0.01).

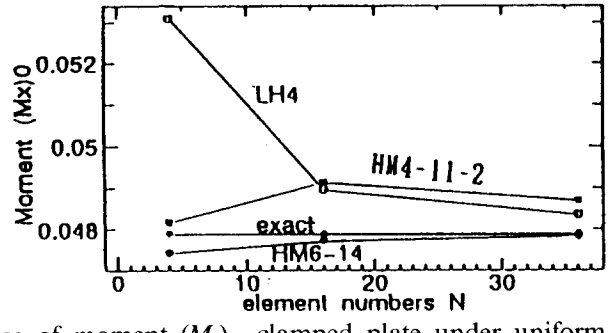

Fig. 12 Convergence of moment $(M_x)_0$, clamped plate under uniform loading (t=0.01).

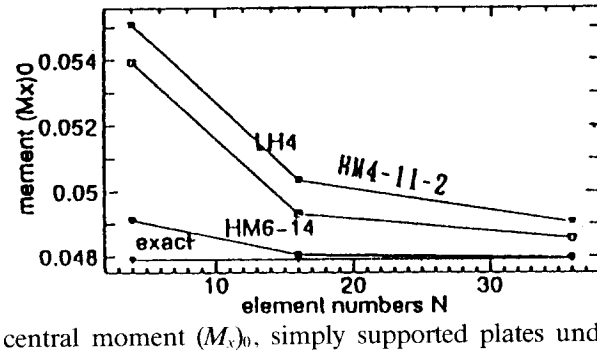

Fig. 13 Convergence of central moment $(M_x)_0$, simply supported plates under uniform roading (t=0.2).

$$= \int_0^h dy \int_0^h [P^T(x, y)DN(x, y) - P^T(x+h, y)DN(x+h, y)]\, dx$$

$$= \int_0^h dy \int_0^h P^T(x, y)[DN(x, y) - DN(x+h, y)]dx$$

$$+ \int_0^h dy \int_0^h [\overline{P}^T(x, y) - (P^T(x+h, y)]\, DN(x+h, y)dx$$

There exists a generalized constant C such that

$$||G^{(1)} - G^{(2)}|| \leq Ch^3$$

Same deductions gives

$$||H^{(1)} - H^{(2)}|| \leq Ch^3 \qquad ||R^{(1)} - R^{(2)}|| \leq Ch^3$$

From Eq. (10), we obtain

$$||\sigma^{(1)} - \sigma^{(2)}|| \leq Ch^3$$

Thus, $\sigma^{(1)} = \sigma^{(2)}$ as $h \to 0$, namely, stress is continuous when the size of mesh is within limit. Therefore, there exist a $h_0 > 0$, stress σ may be expressed by nodes stress when $h \leq h_0$, According to theorems in Zhou and Duan (1993), the hybrid/mixed finite element solution of element HM6-14 is convergent. By the way, it is easy to achieve a convergence element, but it is very difficult to achieve an element with fine qualities and high ratio of convergence.

5. Numerical studies

5.1. Square plate

5.1.1. Convergence of solution

The theories about six-node hybrid/mixed plate bending element have already been introduced in the previous section. In this section, we will illustrate the efficiency of the present element by numerical studies. Let us first introduce the following notations: v-Poisson's ratio, E-elastic modulus, t-thickness, *SS*-simply supported, *CC*-fixed supported, *UL*-uniform loading, *CL*-concentrated loading. Because of its symmetry we consider only the quadrant (Fig. 4 and Fig. 5) of the square plate. The present element yields better results than those by 4-node hybrid/mixed finite element LH4 (Pan 1985) and HM-11-2. Fig. 6~Fig. 13 show the convergence of central displacement, and moments for clamped plate and simply supported plate under uniform loading and concentrated loading.

5.1.2. Solution invariability to distorted mesh situations

W_0, M_x, M_y of element HM6-14 have invariability (shown as Table 2) to distorted mesh situations (Fig. 14).

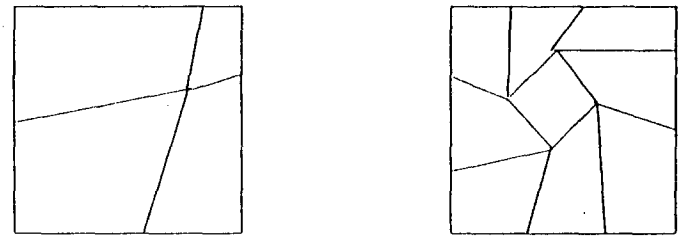

Fig. 14 The invariability of solution to distorted mesh situations.

Table 2 W_0, M_x, M_y to distorted mesh situation

W_0	2×2RM	2×2DM	DM/RM
CCUL	954.0422	973.1744	1.0200538
SSUL	4050.43	3723.626	0.919316

M×B	Exact	3×3DM	Ex./DM
CCUL	−0.0513	−0.054749	0.9370034
SSUL	−0.03246	−0.029098	1.1155406

W_0	Exact	3×3DM	Ex./DM
CCUL	1260	1253.89	0.99515
SSUL	4062	3797.687	0.9349286

M_y0	2×2RM	2×2DM	RM/DM
CCUL	0.0234763	0.0241398	0.9725143
SSUL	0.0498284	0.0573507	0.8688368

$M_{xy}B$	2×2RM	2×2DM	RM/DM
CCUL	−0.034487	−0.041556	0.8298219
SSUL	−0.029821	−0.041373	0.7207841

M_y0	Exact	3×3DM	Ex/DM
CCUL	0.0231	0.022132	1.0437376
SSUL	0.04789	0.042933	1.115459

Note: RM, DM denote regular mesh and distorted mesh, respectively.

Table 3 Results to axial rotation

α	0	15	30	45	60	75	90	180	270
HM/EXACT	1.0261413	1.134577	0.9634548	0.7197784	1.1560468	1.1028649	1.0261413	1.0261413	1.0261413

On the other hand, we don't show the nodes locations in the structure mesh because arrangement & orientation of nodes have few effect on the solutions for HM6-14 element, which will be shown in following section (*5.1.4*).

5.1.3. Invariability to axial rotation

$$x' = x\cos\alpha + y\sin\alpha$$
$$y' = y\cos\alpha - x\sin\alpha$$

Table 3 shows that HM6-14 is almost invariable to axial rotation

5.1.4. Invariability to node positions

Fig. 16 describes different types of 6-node element HM6-14. Results in Table 4 show that HM6-14 has invariability to node positions.

Table 4 Results to node positions

	I	II	III	IV	V	VI	Exact
W_0	1292.938	1292.938	1292.938	1407.377	1292.938	1564.07	1260
$(M_x)_A$	−0.041814	−0.041834	−0.041814	−0.048916	−0.041834	−0.050608	−0.0513
$(M_y)_0$	0.0294317	0.0294317	0.0294317	0.0284562	0.0294317	0.0356148	0.0231

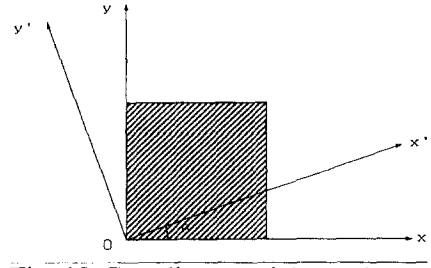

Fig. 15 Coordinate axial rotations.

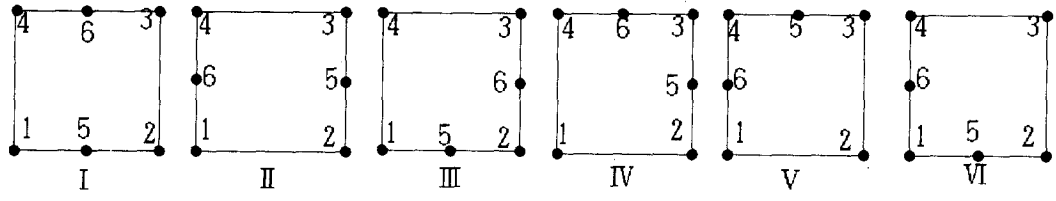

Fig. 16 Different type HM6-14 elements.

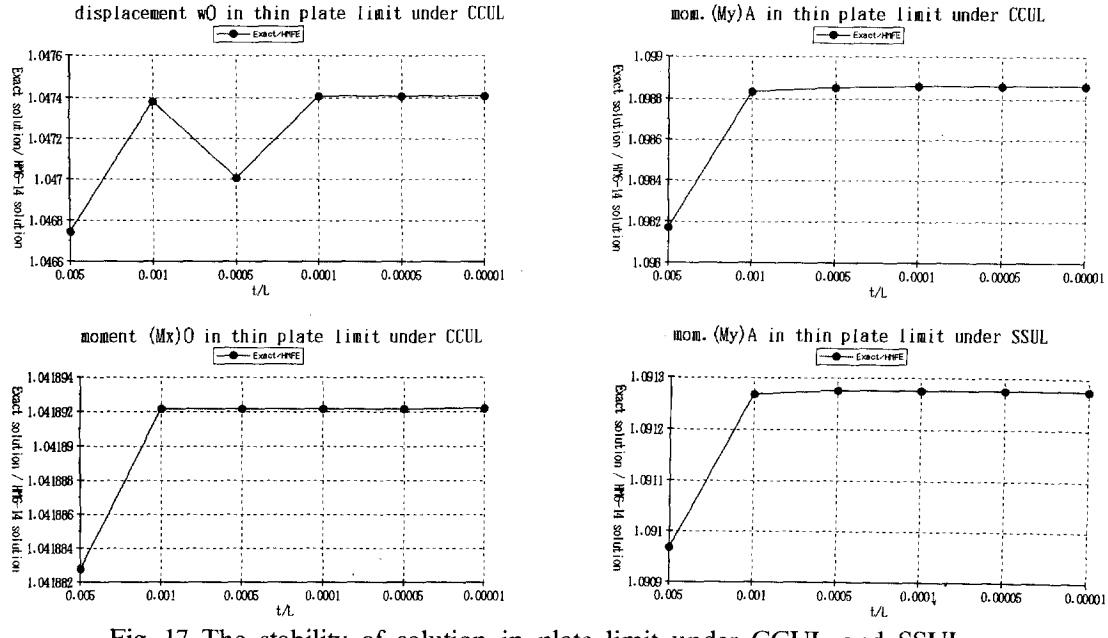

Fig. 17 The stability of solution in plate limit under CCUL and SSUL.

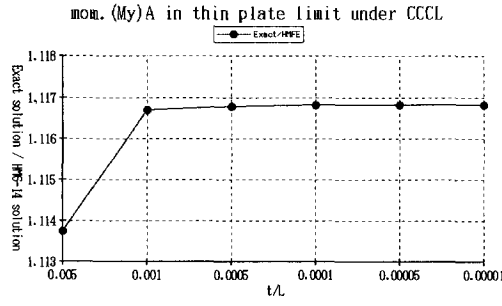

Fig. 18 The stability of solution in plate limit under CCCL.

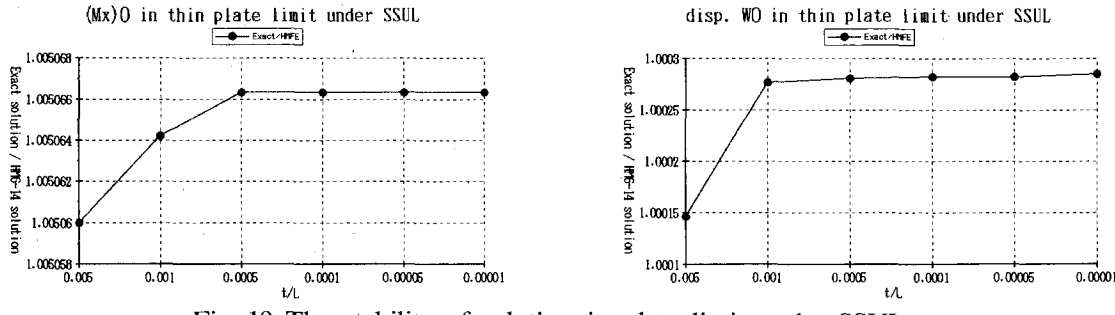

Fig. 19 The stability of solution in plate limit under SSUL.

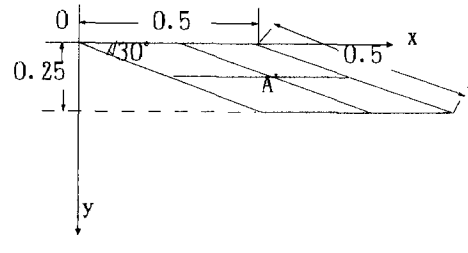

Fig. 20 30° simply supported skew plate
E=10^6, t=0.01, v=0.2 uniform loading: q=1.0.

5.1.5. The stability of solution in thin plate limit conditions

Displacement FEM has "locking" effect while HM6-14 element for hybrid/mixed FEM has none in the thin plate limite, as shown in Figs. 17-19.

5.2. Morley's 30° simply supported skew plate

It is very difficult to obtain acceptable solutious for the Morley's skew plate (Fig. 20) by use of today's large scale general purpose finite element programs. In this case, errors of about

Table 5 Displacement and bending moment M_{max} at the centre of the skew plate.

	W_A	M_{max}
Exact	0.0003582	0.004825
Exact/HM6-14	1.411848	1.00456

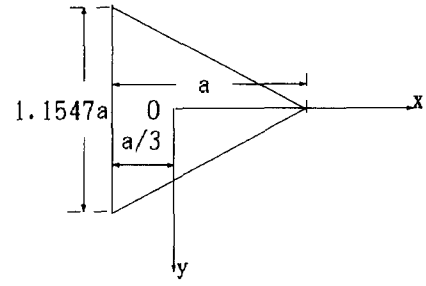

Fig. 21 Triangular plate.

Table 6 Central displacement and moment of triangular plate

	W_0	M_x	M_y
HM6-14	1043.666	0.0310625	0.032435
HM6-14/Exact	1.01444	1.290289	1.347299

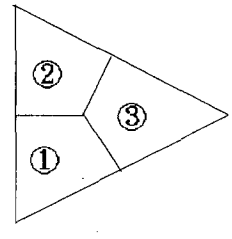

Fig. 22 3-element mesh of triangular plate.

20% may be apparent even if 14×14 meshes are employed. So far, the best way to solve this problem is invoking adaptive FEM or using elements with special qualities. The authors adopt the second way and achieve almost satisfactory results with only a 2×2 mesh (Table 5).

5.3. Triangular plate

Triangular plate is also often used in practical applications. For example, slump in the floor of fuel reservoirs and silos are equilateral triangular plate, so it is necessary to study it. Now

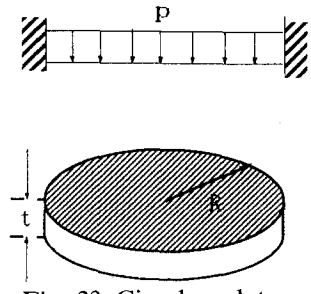

Fig. 23 Circular plate.

Table 7 W_{max} of circular plate

W_{max}	CCUL	SSUL
HM6-14	918.9709	3390.055
HM6-14/Exact	0.9410262	0.85148

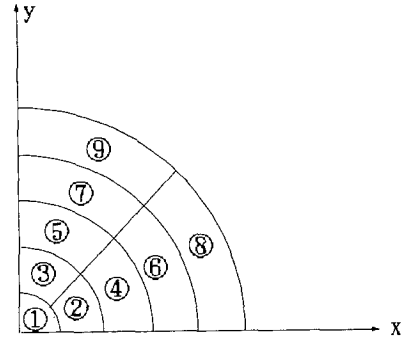

Fig. 24 9-element mesh of circular plate.

consider equilateral triangle plate shown in Fig. 21. It can be seen from Table 6 that the results corresponding to $t/L=0.01$ with HM6-14 under the division shown in Fig. 22 are in close agreement with exact solutions.

5.4. Circular plate

Fig. 23 is a circular plate. Numerical results (Table 7) are satisfactory under the SSUL and CCUL condition and the mesh divided as Fig. 24.

6. Conclusions

A new 6-node hybrid/mixed finite element HM6-14 for the analysis of thin~moderately thick plates has been presented. The presented element possesses many good properties. In general,

the solution accuracy with this element will not be greatly affected when the element shape is distorted from regular geometry. It can provide acceptable results even if coarse meshes are used. In addition, the element has no extra zero-energy modes and shear locking as its thickness approaches the thin plate limit. Numerical studies show the good convergence characteristies of the element. Indeed, an efficient plate bending element has been established which is suitable to the development of adaptive hybrid/mixed FEM due to its transition properties between lower and higher order elements.

References

Masa Hayashi and Takaki Sakaguchi (1993), "Mindin node-strip elements for the bending analysis of thick and thin plate", *Journal of Structural Mechanics and Earthquake Engineering,* **1**(459), 93-101.

Pan, Y. S. (1985), Master Thesis, Southwestern Jiaotong University, Sichuan, China.

Pian, T.H.H. (1964), "Derivation of element stiffness matrices by assumed stress distributions", *AIAA* **7**, 1333-1335.

Pian, T.H.H. and Chen, D.P. (1982), "Alternative way for formulation of hybrid stress elements", *Int. J. Numer. Methods. Eng.,* **18**, 1679-1684.

Pian, T.H.H. and Chen, D.P. and Kang, D. (1983), "A new formulation of hybrid/mixed finite elements", *Comp. and Struct.,* **16**, 81-87.

Pian, T.H.H. and Chen, D.P. (1983), "On the suppression of zero energy deformation models" *Int. J. Num. Meth. Eng.,* **19**, 1741-1752.

Stummel, F. (1980), "The limitations of the patch test", *I.J.N.M.E.,* **15**, 177-188.

Zhong, C. S. (1984), "On the convergence properties of the quadrilateral element of Sander and Beckers", *Math. Comp.,* **42**, 493-504.

Zhou, B. K. and Duan, M. (1993), "Error estimates of h- and p-convergence in multi-field finite elements", *Proceeding of the second Asian-Pacific Conference on Computational Mechanics,* Australia, August.